Simultaneous Control of Au Nanotube Lengths and Pore Sizes with a Single Kind of Polycarbonate Membrane *via* Interfacial Deposition at the Air/Water Interface

Myoungho Pyo,* Jungsook Joo, and Youn Su Jung

*Department of Chemistry, Sunchon National University, Chonnam 540-742, Korea. *E-mail: mho@scnu.ac.kr*
Received March 12, 2007

Au was electrolessly deposited on polycarbonate (PC) membranes (0.1 μm pores) at the air/water interface. It was found that the Au nanotube dimension can be controlled by adjusting the plating temperature and the solution composition. Interfacial deposition of Au at relatively low temperatures (4 ^{o}C) produced long nanotubes, which run through the whole membrane thickness with small openings. Increase of plating temperatures resulted in the decrease of nanotube lengths and Au film thicknesses. It was also disclosed that the inside-diameter of Au nanotubes can be controlled with negligible variations in length by changing the composition of a plating solution.

Key Words : PC membrane, Au nanotube, Electroless deposition, Interfacial deposition

Introduction

Since the preparation of nanostructures through a template-assisted method is relatively straightforward and easy to scale-up, various nanoporous templates have been utilized for the construction of hollow nanotubes or solid nanorods of well defined dimensions over the last decades.[1-6] Templates include inorganic materials such as anodized aluminum oxides[7] and zeolites,[8] organic materials such as track-etched PC membranes[9-12] and regularly ordered polymers,[13] and biological materials.[14]

Template-assisted synthesis of a variety of nanostructures *via* electrochemical and chemical methods has been reported.[1-3,5-6,13] As a result, one can now routinely constrain the growth of desired materials such as metals, semiconductors, and insulators within template channels. Although the electrochemical method has advantages for some cases such as the preparation of segmented nanowires of different components by a sequential deposition,[12,15] it appears that the electroless deposition has been preferred since it does not require metallic coating for electrical contact. In the chemical deposition, the variation of plating times makes it possible to finely control the pore diameter of nanotubes. Complete filling of template channels is also possible by lengthening the reaction time.[9] Utilizing track-etched PC membranes as a template, Martin *et al.* reported various experimental results demonstrating selective transport properties by controlling inside-diameters and surface properties of Au nanotubes.[6,9-11] However, simultaneous control of the length and the pore size with a single kind of membrane was impossible as the length of nanotubes is strictly determined by the membrane thickness.

This paper addresses electroless deposition of Au on track-etched PC membranes at the air/water interface. The formation of Au nanotubes of various lengths and inside-diameters by adjusting plating temperatures and solution compositions is demonstrated.

Experimental

Commercially available PC membranes of 0.1 μm pore diameters (nominal thickness = 6 μm, pore density = 4×10^8 cm^{-2}, SPI-Pore^{TM}) were used as a template. Besides floating membranes on a Au plating solution, Au depositions were carried out *via* the same procedure as described previously by others.[16] Briefly, membranes were sensitized with a methanol/H_2O (50/50, v/v) solution of 0.026 M $SnCl_2$ and 0.07 M CF_3COOH for 15 min. After thorough washing with methanol and water, dried membranes were floated on an ammoniacal $AgNO_3$ solution for 30 sec to yield Ag nanoparticles on membrane faces and pore walls. After washing with copious amounts of water, membranes were dried at ambient overnight. Membranes were then carefully floated on an aq. solution of 7.9 mM Au^+ (diluted from a commercial Au plating solution, Oromerse SO Part B, Technic, Inc.) and 0.127 M Na_2SO_3 (Aldrich). Maintaining temperatures constant, HCHO was added to be 0.625 M and the reaction proceeded for 15 hrs. Membranes were then dipped in a *ca*. 20% HNO_3 solution for 6 hrs and heat-sealed at 150 ^{o}C for 12 hrs.

Permeation tests were performed in an H-cell. One compartment was loaded with a solution of 0.1 M methyl viologen (MV^{2+}) dichloride and 0.1 M NaCl and the other with a MV^{2+}-free solution of 0.1 M NaCl. Permeation of MV^{2+} with time was electrochemically monitored utilizing a potentiostat (EC Epsilon) equipped with a Au button (working, geometrical area = 0.02 cm^2), a Ag wire (reference), and a Pt plate (counter).

Au nanostructures were examined by contact-mode atomic force microscopy (Nanoscope E, DI), scanning electron microscopy (JSM T-330A, JEOL), and field emission scanning electron microscopy (XL30S FEG, Philips).

Results and Discussion

Au deposition on PC membranes at the interface was

carried out at 4, 25, 50, and 75 °C. After Au deposition, the solution-contacting face (SCF) of membranes exhibited visual similarity with a typical color of Au regardless of the deposition temperature, but the air-contacting face (ACF) became dark brown from yellowish brown as the temperature was increased from 4 °C to 75 °C. In addition, the electric conduction along with ACF was observed only for the membrane made at 4 °C. The other 3 samples showed no electric conduction. However, it does not mean that ACF of the membrane made at 4 °C was fully covered with a Au film. After removing the Au film of SCF by mechanically polishing with an ethanol-wetted cotton swab, the electric conduction along with ACF was no longer observed, indicating that Au was not deposited on ACF. This was further confirmed by the fact that ACF of all 4 samples required metallic coating for scanning electron microscopy (SEM) measurements. These color and conductance differences suggest that the dimension of Au nanostructures prepared at the interface is influenced by the plating temperature. It should be mentioned that, as far as Au deposition is carried out at the interface, pretreatments (sensitization and Ag particle formation) of membranes either by floating on or dipping in solutions give the identical results.

In order to compare the extent of Au deposition within pores, the Au-coated membranes were placed in aqueous solutions of 0.1 M NaCl and capacitances measured from cyclic voltammograms (CVs) at 0.1 Vs^{-1}.[16] Au surface areas per unit area of membrane face (no pore wall area was included.) were summarized in Table 1. Considerably greater surface areas than 1.0 cm^2 for all samples indicate that nanotubes, rather than nanorods, were produced. If nanorods were formed, Au surface areas should be about 1.0 cm^2 irrespective of the deposition temperature. Large variations of the surface area suggest again that the length and/or the inside-diameter of Au nanotubes depend on the deposition temperature.

In order to examine the surface feature of Au-deposited membranes without metallic coating, we utilized contact-AFM instead of SEM. Figure 1 shows AFM images of ACF and SCF (denoted by subscript a and s, respectively) of Au-coated membranes at (A) 4, (B) 25, (C) 50, and (D) 75 °C. Besides $1A_a$, AFM images of $1B_a$, $1C_a$, and $1D_a$ show similar pore diameters of *ca.* 0.1 μm. Deviation of $1A_a$, exhibiting slightly smaller pore diameters, is due to nanotubes reaching ACF as mentioned above. AFM images of SCF, on the other hand, indicate that the pore diameter becomes greater as the increase of deposition temperatures. While the pores seem to be clogged at 4 °C ($1A_s$), SCF of a Au-deposited membrane at 75 °C exhibits the opening of *ca.* 40 nm ($1D_s$).

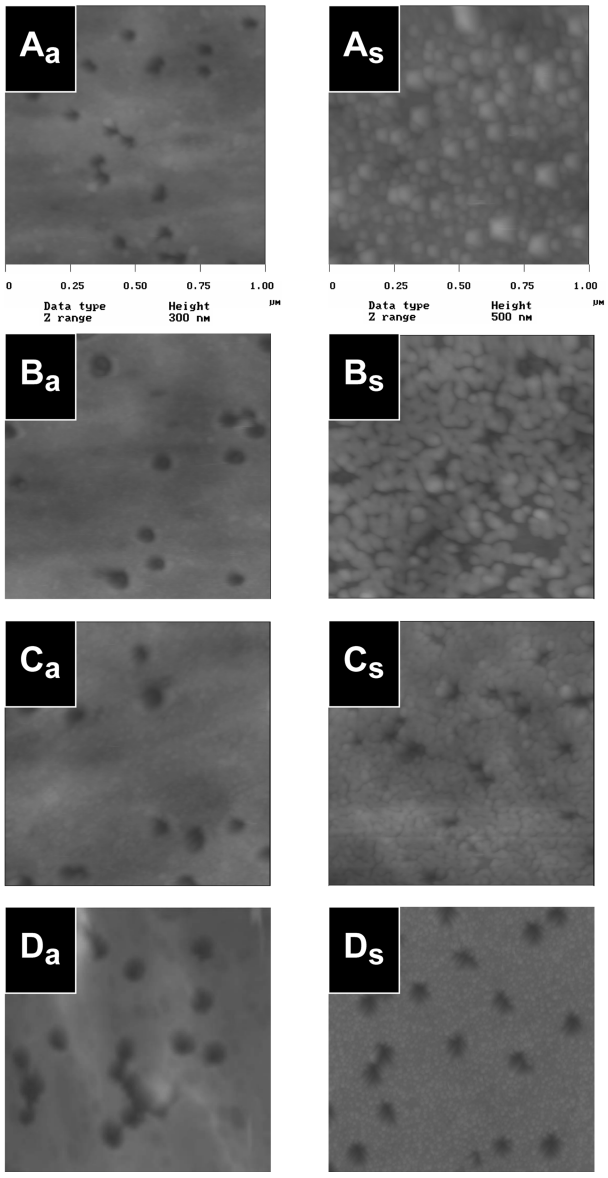

Figure 1. Contact-AFM images of Au-deposited membranes at (A) 4, (B) 25, (C) 50, and (D) 75 °C. Subscript a and s indicate ACF and SCF, respectively.

Although the difference of pore openings of SCF suggests the possibility of a thin film formation with raising the

Table 1. Au surface areas and nanotube dimensions prepared at the interface

Au deposition temperature (°C)	[a]Capacitance (μF) /unit area of membrane face (cm^2)	[b]Au surface area (cm^2) /unit area of membrane face (cm^2)	[c]Au nanotube dimension (μm)		[d]Roughness of Au films
			Length	Pore size	
4	311	14.8	6.4	0.020	5.7
25	202	9.6	2.2	0.042	4.4
50	133	6.3	1.4	0.054	3.2
75	64	3.0	0.7	0.067	1.9

[a]Double layer capacitance was measured from CVs in 0.1 M NaCl at 0.1 Vs^{-1}. [b]Au capacitance of 21 μFcm^{-2} was used.[16] [c]obtained from SEM and FESEM images of Figure 3. [d] roughness = (Au surface area calculated from capacitance)/(geometrical area calculated from dimension)

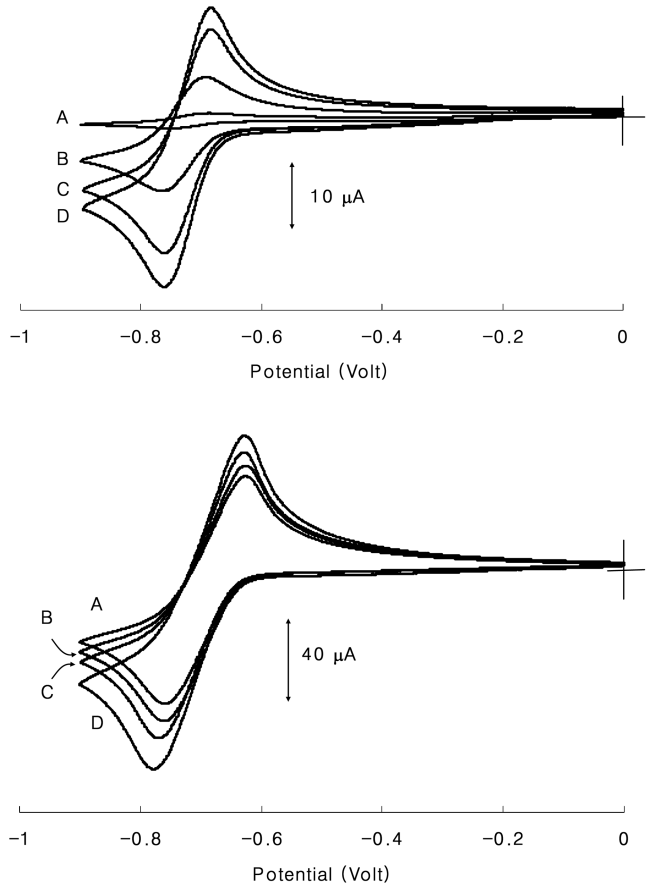

Figure 2. CVs of MV^{2+} diffused, from a solution containing 0.1 M MV^{2+} and 0.1 M NaCl to MV^{2+}-free NaCl solution, through Au nanotubes prepared at (A) 4, (B) 25, (C) 50, and (D) 75 °C (top) before and (bottom) after removal of a Au film on SCF. Scan rate = 0.1 Vs^{-1}.

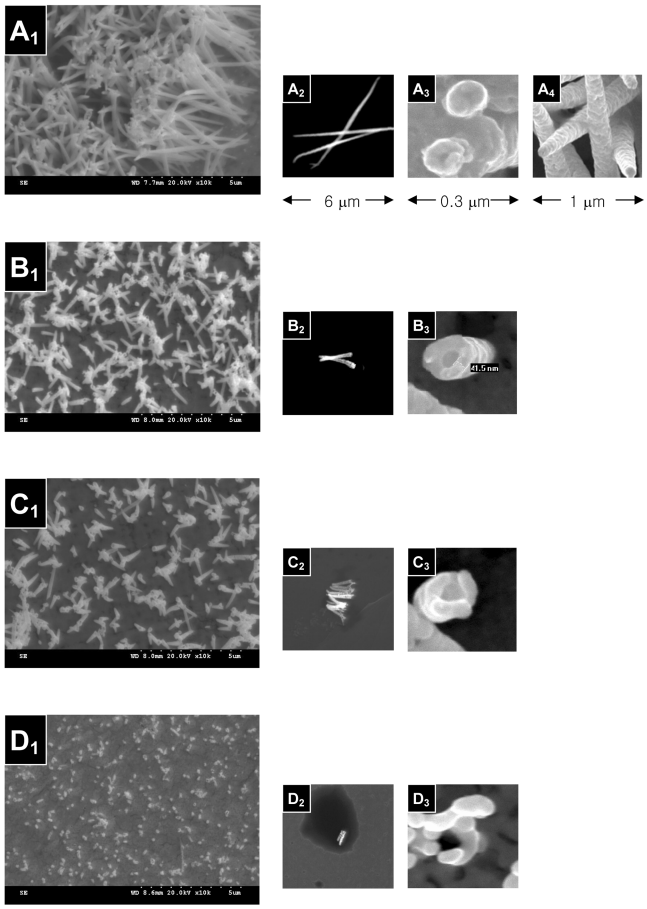

Figure 3. SEM and FESEM images of Au nanotubes prepared at (A) 4, (B) 25, (C) 50, and (D) 75 °C.

deposition temperature, it does not necessarily mean that the inside-diameter of nanotubes also varies with temperatures. In order to tackle this point, we compared the amounts of MV^{2+} permeated through membranes before and after removal of Au films on SCF. Figure 2 (top) shows CVs of MV^{2+} permeated for 6 hrs through as-made membranes. It is not surprising that the redox peak heights of MV^{2+} increase from A to D since the amounts of MV^{2+} permeated is directly related to the pore openings of SCF. This was compared with CVs of MV^{2+} permeated through membranes with bare SCF (Figure 2 (bottom)). Although the peak heights exhibit similar trends, the amounts of MV^{2+} are considerably greater than those with as-made membranes. Note the difference of current scale in Figure 2. Significant increase of the amounts of MV^{2+} implies that preferential deposition of Au on SCF occurs, but does not affect the inside-diameter of nanotubes even in the vicinity of SCF. This behavior is different from the result addressed by Yamada *et al.*,[17] who showed that a Au film with a uniform thickness is formed during electroless Au deposition in a solution.

In order to directly compare the length of nanotubes, SEM images were taken after dissolving out PC by carefully dropping CH_2Cl_2 onto ACF. Figure $3A_1$-$3D_1$ show that the deposition temperature greatly affects the length of nanotubes. Interfacial deposition at 4 °C produces the longest nanotube, which appear to line the whole pore walls. The increase of the deposition temperature results in the reduction of the length. This behavior can be seen more clearly, in Figure $3A_2$-$3D_2$, for which PC membranes were dissolved and ultrasonicated in CH_2Cl_2 after mechanically removing a Au film on SCF. The length of nanotubes prepared at 4, 25, 50, and 75 °C was (A_2) 6.4, (B_2) 2.2, (C_2) 1.4, and (D_2) 0.7 μm respectively. Figure $3A_2$ also shows tapered ends which result from cigar-shaped channels of a template.[18] A FESEM image of tube ends of an ACF side was illustrated in Figure $3A_4$. As expected, nanotubes demonstrate no indication of a Au film on ACF as well as a tapered structure. The pore size of nanotubes was also examined. FESEM images in Figure $3A_3$-$3D_3$ show that the diameter of openings is increased from (A) *ca.* 0.020 μm to *ca.* (B) 0.042, (C) 0.054, and (D) 0.067 μm. Note that the outside-diameters of nanotubes of Figure $3B_3$, $3C_3$, and $3D_3$ are greater than 0.1 μm.

The dimension of the nanotubes was summarized in Table 1. Utilizing the inside-diameter and the length in Table 1 along with a nominal pore density of 4×10^8 cm^{-2} of a PC membrane, the geometrical area of Au was calculated. The geometrical area per unit area of a membrane face was

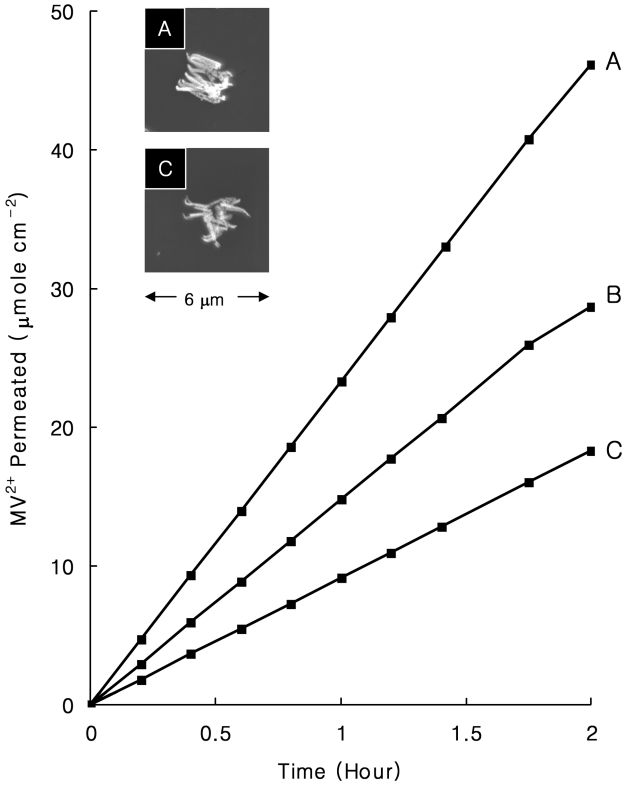

Figure 4. Amounts of MV^{2+} permeated through Au nanotubes prepared on solutions of [Au^+] = (A) 32, (B) 7.9, and (C) 4.0 mM at 25 °C. Insets show corresponding SEM images of nanotubes. For a SEM image corresponding to B, refer to B_2 of Figure 3.

decreased from 2.6 cm^2 at 4 °C to 2.2, 2.0, and 1.6 cm^2 as the increase of deposition temperature. The roughness of Au (*i.e.*, the ratio of the surface area obtained from capacitance to the geometrical area) was listed in the rightmost column of Table 1. Reduction of the surface roughness of Au films at relatively high temperatures corresponds to the smooth surfaces shown in Figure $1C_s$ and $1D_s$.

The control of the inside-diameter of nanotubes, keeping the length variation minimized, is also possible by adjusting Au^+ concentrations of a plating solution. Au films on SCF were removed after deposition and cathodic peak currents of CVs, due to MV^{2+} permeation, were monitored with time. Peak currents were converted to the concentration of MV^{2+} by using the Randles-Sevick equation. Figure 4 shows the amounts of MV^{2+} permeated through nanotubes prepared in [Au^+] = (A) 32, (B) 7.9, and (C) 4.0 mM at 25 °C. It is obvious that the diffusion of MV^{2+} becomes more hampered through the nanotube prepared in a more diluted solution of Au^+. Since the SEM images indicate the similar nanotube length (insets in Figure 4), the differences in the amounts of MV^{2+} are ascribed to the decrease of the pore size with a dilution of [Au^+].

Conclusions

Deposition of Au at the interface produces the nanotube of various lengths and pore sizes, controlled by the temperature and the concentration of Au^+, indicating that the preparation of Au nanotubes of various dimensions with a single kind of template is possible. As the increase of plating temperatures, interfacial deposition results in the formation of long nanotubes with small pores. Minimizing the length variation, the inside-diameter of nanotubes can also be controlled by adjusting the concentration of Au^+.

Acknowledgment. This work was supported by the Korea Research Foundation Grant funded by the Korean Government (MOEHRD, Basic Research Promotion Fund) (KRF-2006-521-C00080).

References

1. Hernandez-Velez, M. *Thin Solid Films* **2006**, *495*, 51.
2. Sung, D. D.; Choo, M. S.; Noh, J. S.; Chin, W. B.; Yang, W. S. *Bull. Korean Chem. Soc.* **2006**, *27*, 1159.
3. Li, C. *Bull. Korean Chem. Soc.* **2006**, *27*, 991.
4. Hoa, M. L. K.; Lu, M.; Zhang, Y. *Adv. Colloid Interface Sci.* **2006**, *121*, 9.
5. Díaz, D. J.; Williamson, T. L.; Gua, X.; Sood, A.; Bohn, P. W. *Thin Solid Films* **2006**, *514*, 120.
6. Harrell, C. C.; Lee, S. B.; Martin, C. R. *Anal. Chem.* **2003**, *75*, 6861.
7. Zhao, S.; Roberge, H.; Yelon, A.; Veres, T. *J. Am. Chem. Soc.* **2006**, *128*, 12352.
8. Yang, Z.; Xia, Y.; Sun, X.; Mokaya, R. *J. Phys. Chem. B* **2006**, *110*, 18424.
9. Nishizawa, M.; Menon, V. P.; Martin, C. R. *Science* **1995**, *268*, 700.
10. Martin, C. R.; Nishizawa, M.; Jirage, K.; Kang, M. *J. Phys. Chem. B* **2001**, *105*, 1925.
11. Gasparac, R.; Mitchell, D. T.; Martin, C. R. *Electrochim. Acta* **2004**, *49*, 847.
12. Reynes, O.; Demoustier-Champagne, S. *J. Electrochem. Soc.* **2005**, *152*, D130.
13. Hoa, M. L. K.; Lu, M.; Zhang, Y. *Adv. Coll. Interf. Sci.* **2006**, *121*, 9.
14. Zhang, B. J.; Davis, S. A.; Mendelson, N. H.; Mann, S. *Chem. Commun.* **2000**, *9*, 781.
15. Park, S.; Lim, J.-H.; Chung, S.-W.; Mirkin, C. A. *Science* **2004**, *303*, 348.
16. Menon, V. P.; Martin, C. R. *Anal. Chem.* **1995**, *67*, 1920.
17. Yamada, K.; Gasparac, R.; Martin, C. R. *J. Electrochem. Soc.* **2004**, *151*, E14.
18. Apel, P. Yu.; Blonskaya, I. V.; Dmitriev, S. N.; Orelovitch, O. L.; Sartowska, B. *J. Membr. Sci.* **2006**, *282*, 393.